International Journal of Pharmaceutics 420 (2011) 282–289

Contents lists available at SciVerse ScienceDirect

International Journal of Pharmaceutics

journal homepage: www.elsevier.com/locate/ijpharm

# Release and cellular acceptance of multiple drugs loaded silk fibroin particles

Pujiang Shi [a], James C.H. Goh [a,b,*]

[a] Department of Orthopedic Surgery, National University of Singapore, 10 Lower Kent Ridge Road, Singapore 119260, Singapore
[b] Division of Bioengineering, National University of Singapore, Singapore

ARTICLE INFO

*Article history:*
Received 27 June 2011
Received in revised form 5 August 2011
Accepted 31 August 2011
Available online 6 September 2011

*Keywords:*
Silk fibroin
Particle
Delivery
Release
Osteoblast

ABSTRACT

In this article, silk fibroin particles with average diameter of 980 nm were fabricated via self assembly. Exceptional loading efficiency and release patterns of hydrophobic and protein drugs were observed. Furthermore, smoother release patterns were observed with increase loading of the hydrophobic and protein model drugs, only about 23% FITC–BSA and 34% RhB were released from the silk particles at their highest corresponding loading in 50 days. Most importantly, osteoblasts' viability was augmented during co-culture with silk fibroin particles, as shown by Alamar Blue assay. Attachment of the particles and delivery of model drugs to cells were confirmed by fluorescence images and flow cytometry. Hence, the silk fibroin particles could be potential biomaterial for application in controlled release and pharmaceutics.



## 1. Introduction

There were a lot of attentions on silk fibroin, due to its outstanding biocompatibility, composition of special proteins, excellent mechanical stability and sustainable degradability, which could be regarded as significant advantages compared with the properties of other synthetic and natural materials (Shi et al., 2009; Wenk et al., 2008). Widespread applications of silk fibroin includes: (1) as a scaffold to support the growth and differentiation of several types of cell (Fan et al., 2009; Min et al., 2004; Weska et al., 2009; Zhao et al., 2009); (2) as a carrier for cytokines and drugs to achieve sustain release, tissue modulation and anti-inflammation (Hofmann et al., 2006).

Most current researches on silk fibroin particles focused on the preparation techniques. Slotta et al. (2008) reported that silk fibroin particles self-assembled in the presence of potassium phosphate with concentration no less than 400 mM. However, Lammel et al. (2010) found that silk fibroin particles formed in no less than 0.75 M potassium phosphate solution, and the hydrophobic model drug (rhodamine B) released quickly with high burst release at the first 3 h. Silk fibroin microspheres with controllable diameters could be prepared by microfluidic device, as described by Breslauer et al. (2010). The use of other organic solvents to manufacture silk fibroin particles was also reported, such as ethyl acetate, diethyl ether, dichloromethane and chloroform, however the conditions of fabrication of silk fibroin particles in these cases were hash and uncontrollable (Baimark et al., 2010). Polyvinyl alcohol (PVA) and ethanol have been utilized to manufacture silk particles independently, and their appearances and sizes can be controlled (Cao et al., 2007; Wang et al., 2010). Silk fibroin microspheres could also be made by spraying the solution into liquid nitrogen, their size distribution varied from 100 to 500 μm, too big for cellular delivery (Wenk et al., 2008). Lipid templates to manufacture silk fibroin particles were also reported by Wang et al. (2007) however, the templates were not stable under organic solvent treatment. Wang et al. (2010) found that the silk particles were better for hydrophobic drugs loading and release. Moreover, silk fibroin microspheres were found to have promising absorption ability for bovine serum albumin (BSA), with higher quantity of BSA being absorbed by smaller size silk particles (Srisuwan et al., 2009).

The ultimate goals for the fabrication of silk particles should be their application, included delivering therapeutic agents to pathological sites, increasing targeting efficiency and alleviating side effects, and particles accumulation in normal tissue and its effects (Mathur and Gupta, 2010). In this article, silk fibroin particles were fabricated via self assembly, model drugs including rhodamine B (RhB; 479 Da), rhodamine B isothiocyanate–dextran (RITC–Dextran; 10,000 Da) and fluorescein isothiocyanate labelled bovine serum albumin (FITC–BSA, 66,000 Da) were loaded on these particles. Loading efficiency, release property and delivery of these model drugs to cells were investigated. Various release behaviors and the best fitted model drugs, in terms of their hydrophilicity, for silk particles were investigated.

* Corresponding author at: Division of Bioengineering, National University of Singapore, 9 Engineering Drive 1, Singapore 117575, Singapore. Tel.: +65 65161911; fax: +65 68723069.
*E-mail address:* biegohj@nus.edu.sg (J.C.H. Goh).

0378-5173/$ – see front matter © 2011 Elsevier B.V. All rights reserved.
doi:10.1016/j.ijpharm.2011.08.051

## 2. Materials and methods

### 2.1. Materials

Model drugs RhB (479 Da), RITC–Dextran (10,000 Da), FITC–BSA (66,000 Da), calcium chloride, poly vinyl alcohol (PVA, 85000–124000 Da) and other chemicals used in this study were purchased from Sigma–Aldrich. Ultrapure water from the Milli-Q system (Synthesis, A10) was used.

### 2.2. Silk purification

Bombyx mori silk (Silk innovation center, Thailand) was degummed in 0.02 M $NaHCO_3$ solution at 90 °C for 1.5 h to completely remove sericin. Then the silk solution was obtained by dissolving sericin-free silk fibers in to a ternary solvent system of $CaCl_2/CH_3CH_2OH/H_2O$ (1:2:8 in molar ratio) followed by dialysis (Min et al., 2004). Finally, 6% (w/v) silk solution was prepared and stored at 4 °C for further application.

### 2.3. Preparation of silk particles

Briefly, silk fibroin particles were prepared via self assembly. 100 μl silk fibroin solution was thoroughly mixed with 40 μl ethanol, then vortex for 10 s. Two milliliters PVA solution was then added to the silk/ethanol mixture and vortex for another 10 s. The ternary solution was finally placed into a freezer for 24 h before collection of the silk particles by centrifugation.

### 2.4. Loading silk particles

Drug loading of silk particles was conducted as follows: specific amounts of model drugs were mixed with silk fibroin solution, and then drug loaded silk fibroin particles were prepared as described in Section 2.3. Subsequently the particles were washed three times, and the supernatants were collected and analyzed for residual drug concentration by UV–vis analysis. For FITC–BSA, measurement wavelength was 479 nm (Schacht et al., 2006). For RhB as well as RITC–Dextran, after full spectral absorption scan (NanoDrop, ND1000 spectrophotometer, Thermo Scientific, USA), their measurement wavelengths were set at 554 nm and 557 nm, respectively.

Standard calibration curves for model drugs were used for drug quantification ($r^2 > 0.99$). Drug concentration of sample supernatants was used to calculate the amount of drug incorporated in the silk particles. All experiments were performed in triplicate. Encapsulation and loading efficiency were calculated using Eqs. (1) and (2), respectively:

$$\text{Encapsulation efficiency (w/w\%)} = \frac{\text{amount of model drug in silk particles}}{\text{model drug initially added}} \times 100 \quad (1)$$

$$\text{Loading (w/w\%)} = \frac{\text{amount of drug in silk particles}}{\text{amount of silk particles}} \times 100 \quad (2)$$

### 2.5. Release of drug from silk particles

Drug loaded silk particles were suspended in 1 ml PBS (pH 7.4) with constant shaking. Each vial contained 30 mg of drug loaded silk particles. The solvent was periodically aspirated and replaced with fresh PBS (pH 7.4). The drug content in the PBS was analyzed as described in Section 2.4.

### 2.6. Release kinetics

The kinetics of dissolution was examined by Higuchi, Korsmeyer–Peppas and Weibull models, which represented 3 independent systems that described release profiles for particles, namely diffusion controlled system, swelling controlled system and erosion controlled system (Arifin et al., 2006).

Higuchi model:

$$F = K_H\sqrt{t} \quad (3)$$

Higuchi described drug release as a diffusion process based on the Fick's law, square root time dependent, and this relation could be applied to describe drug dissolution from several types of modified release pharmaceutical dosage forms (Costa et al., 2001). $F$ represented the fraction of drug dissolved in time $t$, and $K_H$ was the Higuchi dissolution constant.

Korsmeyer–Peppas model:

$$\frac{M_t}{M_\infty} = Kt^n \quad (4)$$

It was a semi-empirical equation based on power-law expression to describe the drug release from swelling-controlled systems (Arifin et al., 2006). $M_t/M_\infty$ was fractional release at time ($t$), $k$ was a constant and $n$ was the diffusional exponent.

Weibull model:

$$\frac{M_t}{M_\infty} = 1 - \exp\left[\frac{-(t - t_{lag})^b}{t_{scale}}\right] \quad (5)$$

In Weibull equation, $t_{lag}$ was the lag time before drug release took place, $t_{scale}$ was the time scale of the release process, and $b$ controlled the shape of the release curve. In case of $b > 1$, S-shaped curve; $b = 1$, exponential curve and $b < 1$, parabolic curve with high initial slop followed by an exponential decay (Arifin et al., 2006).

Adjusted coefficient of determination ($R^2_{adjusted}$ or $R_{sqr-adj}$):

$$R^2_{adjusted} = 1 - \frac{n-1}{n-p}(1 - R^2)$$

This equation was used to determine the most appropriate model to describe the dissolution data, $n$ was the number of dissolution data points, $p$ was the number of parameters in the model and $R^2$ was the coefficient of determination (Costa et al., 2001).

### 2.7. Characterization

#### 2.7.1. UV–vis-spectrometry

Ultraviolet–visible spectrometry (Microplate reader, Infinite M200, Tecan, Switzerland) was employed for the determination of drug concentration in supernatants as a basis for the calculation of loading efficiency and release profile. Calibration curves for all model drugs were obtained by using nine distinctive concentrations of all stock solutions.

#### 2.7.2. Scanning electron microscopy (SEM)

Silk particles after lyophilization were added directly on top of conductive tapes mounted on SEM sample stubs. The samples were sputtered with platinum. The morphologies of silk particles were investigated using a FEI XL30FEG (FEI Company of USA, The Netherlands).

#### 2.7.3. Particle size analysis

Silk particles fabricated in Section 2.3, were centrifuged and washed for 3 times to clear PVA and ethanol. Finally, the silk particles were resuspended in Milli-Q water and analyzed by high performance particle size analyzer (HPPS, Malvern Instruments Ltd., UK).

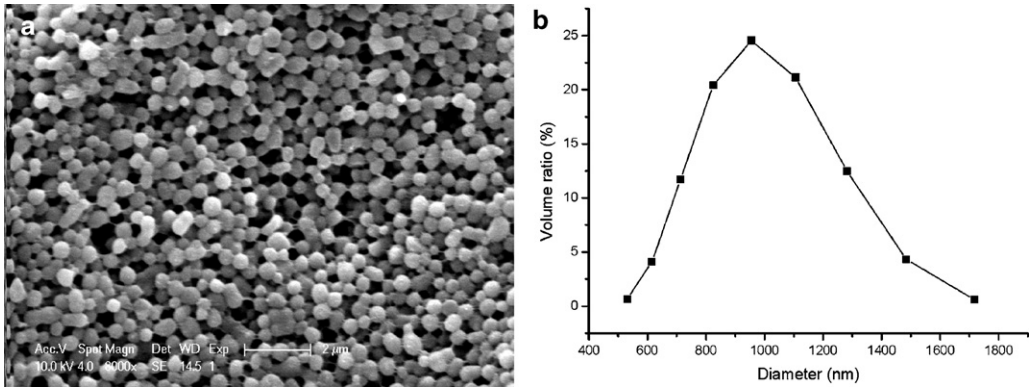


**Fig. 1.** SEM image of silk fibroin particles (a) and their size distribution (b).

*2.7.4. Light microscopy*

For model drugs loaded silk particles, 100 μl silk particles solution were placed on glass slide under Carl Zeiss apotome microscope (Carl Zeiss, Jene, Germany). Images were taken with installed software.

*2.7.5. Confocal microscopy*

The RhB, RITC–Dextran and FITC–BSA loaded silk particles were observed by Nikon FV 1000 microscope, at an excitation wavelength of 555 nm and an emission wavelength of 580 nm for RhB and RITC–Dextran. For FITC–BSA, the excitation and emission wavelengths were set at 495 nm and 521 nm individually. Several *xy* scans with an optical slice of 100 nm were stacked along the *z*-direction to obtain a 3D image and the crossection of silk particles and the distribution of encapsulated RhB, RITC–Dextran and FITC–BSA was visualized.

*2.8. In vitro evaluation*

*2.8.1. Osteoblasts/silk particles co-culture*

Osteoblasts were obtained from New Zealand White rabbit using a published protocol approved by NUS Institutional Animal Care and Use Committee, National University of Singapore (Cao et al., 2006). Briefly, cervical bone of New Zealand White rabbit was aseptically taken out, washed by Hank's solution 3 times, and digested with 0.25% trypsin for 15 min. Then, cells were cultured in a plastic culture flask until nearly confluent. Osteoblasts (P5) were seeded in 24 wells plate, 0.1 million cells per well. Cells were cultured in a complete medium, comprising DMEM-low glucose, 10% FBS and 1% penicillin–streptomycin, which was replaced twice every week. After 6 h cell seeding, 15 mg silk particles in 1 ml PBS were added in the 6 wells separately; and 1 ml blank PBS was added in the other 6 wells respectively, as control group.

*2.8.2. Cell viability and proliferation studies*

Cell viability and proliferation were monitored using Alamar Blue (Molecular Probes, Invitrogen Corporation) dye reduction assay ($n = 6$). 1 ml test medium consisted of 10% Alamar blue, 5% FBS was added in each well for 3 h, then test medium was aspirated and centrifuged at 4000 × *g* for 30 min to get rid of any silk particles in the medium, and absorbance at 570 and 600 nm was measured in a microplate reader (Infinite M200, Tecan, Switzerland), following the vendor's protocol.

*2.8.3. Light microscopy*

Osteoblasts cultured with RhB and FITC–BSA loaded particles on glass plates, after 24 h osteoblasts were fixed in 2% paraformaldehyde, and observed under Carl Zeiss apotome microscope.

*2.8.4. Flow cytometry*

Osteoblasts at passage 5 were cocultured with RhD and FITC–BSA loaded silk fibroin particles. After 24 h, cells were detached, centrifuged and resuspended in PBS containing 1% FBS. And then, the cells suspension was fixed in 2% paraformaldehyde for 15 min, followed by flow cytometry analysis to analyze the drugs delivery to the target cells.

## 3. Results and discussions

*3.1. Appearance and size distribution of silk fibroin particles*

As can be seen in Fig. 1a, the appearance of silk particles was round with tiny amount of particles aggregated together via silk fiber. PVA was employed in the reaction as an emulsifier to prevent agglomeration of silk particles; however, it could not stop fiber formation due to their really small size. Particle size distribution was between 500 nm and 1.5 μm (Fig. 1b), and their average diameter was 980 nm. The size distribution of silk particles as quantitated by SEM image varied from 300 nm to 1.3 μm, and the average diameter was 686.5 nm (data was obtained by ImageJ software; version 1.44). Obviously, there were deviations present between the data of HPPS and the data of SEM image, which probably caused by shrinking of the particles during dehydration process in the sample preparation for SEM.

*3.2. Loading and release*

*3.2.1. Loading*

As model drugs, FITC–BSA, RITC–Dextran and RhB were mixed with silk fibroin solution prior to particle preparation. FITC–BSA emitted green fluorescence, and RITC–Dextran and RhB emitted red fluorescence after excitation. Therefore, the distribution of conjugated drug molecules in silk particles could be monitored and their loading and release was readily determined. The three model drugs have distinctive molecular weights (66,000, 10,000 and 479 Da, respectively), hydrophobicities (RhB > FITC–BSA > RITC–Dextran) and surface charges (FITC–BSA: negative; RITC–Dextran: neutral; RhB: positive) (Wang et al., 2010). Along with the increase of actual loading of FITC–BSA, their encapsulation efficiencies decreased respectively. After mixing more FITC–BSA with silk, additional drugs were interacted with silk due to hydrophobic interactions as well as electrostatic binding. However, most drugs remained outside the particles without any interactions with silk, which decreased the encapsulation efficiency dramatically. For example, the actual loading of FITC–BSA was at 0.27% corresponding to 80.06% encapsulation efficiency which was much higher than that of silk particles loaded with more FITC–BSA whose encapsulation efficiency decreased, as can be seen in table of Fig. 2. Moreover,

| | Property | Initial loading (mg/mg silk, %) | Encapsulation efficiency (%) | Actual loading (mg/mg silk, %) |
|---|---|---|---|---|
| FITC-BSA | Hydrophobic Negative charge | 0.3 | 80.06 | 0.27 |
| | | 10 | 41.82 | 4.65 |
| | | 25 | 39.24 | 10.91 |
| | | 35 | 34.46 | 13.34 |
| RITC-Dextran | Hydrophilic Neutral | 0.3 | ≈0 | ≈0 |
| | | 35 | 2.68 | 1.04 |
| RhB | Hydrophobic Positive charge | 0.3 | 45.87 | 0.153 |
| | | 35 | 30.81 | 11.99 |

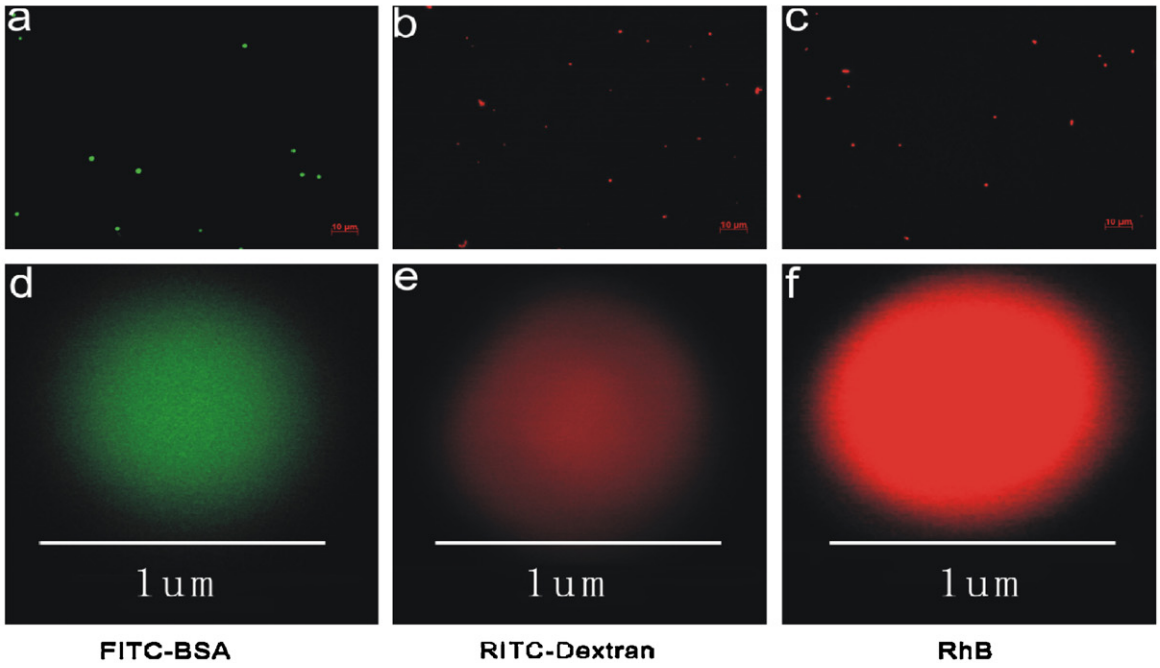


**Fig. 2.** Loading and distribution of model drugs in silk particles: phase contrast microscopy (Apotome, Carl Zeiss, USA) images were made on the spheres suspended in aqueous solution. (a–c), low magnification images, bar = 10 μm. High magnification images were made by confocal microscopy (d–f), bar = 1 μm. The table above showed drug encapsulation efficiency and actual loading determined by measuring the amount of drug remained in the supernatant fractions after centrifugation.

referred to the other hydrophobic model drugs in Fig. 2, their properties such as the encapsulation efficiencies of RhB behaved similarly to FITC–BSA after actual loading went up. Meanwhile, encapsulation efficiency of hydrophilic drugs like RITC–Dextran actually went up with increased loading, behaved contrarily to that of hydrophobic drugs (FITC–BSA and RhB).

Both FITC–BSA and silk were protein and shared similar structure including hydrophobic and hydrophilic parts. High molecular

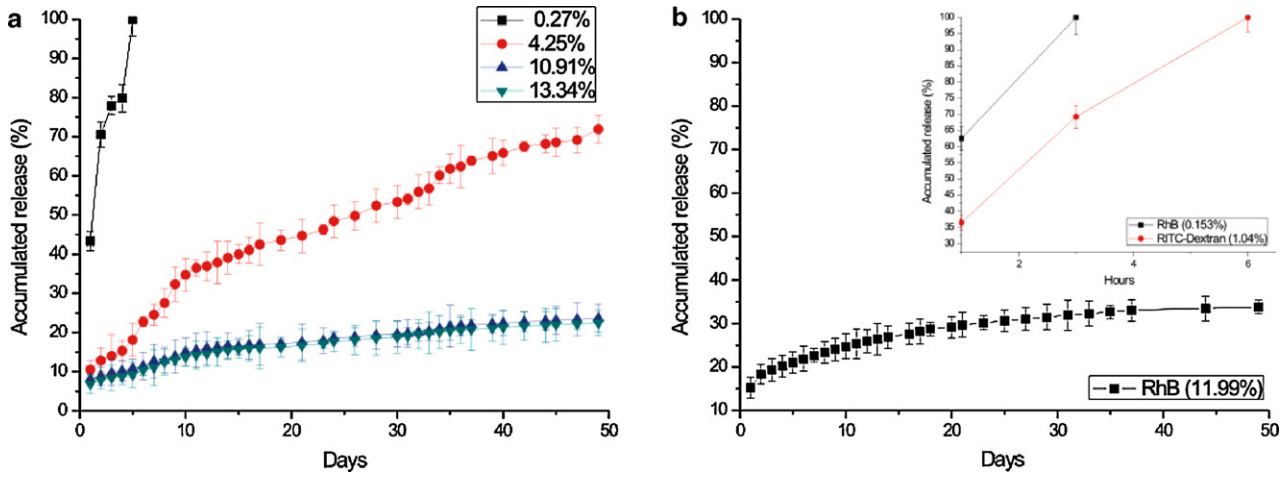


**Fig. 3.** Release from silk fibroin particles. (a) Release of FITC–BSA at various loading; (b) release of RhB and RITC–Dextran from silk fibroin particles at several loading.

affinities promised outstanding encapsulation efficiency up to 80.06%, compared with that of RhB which was also hydrophobic drug. In the mean time, the molecular weight of RhB (479 Da) being much lower than that of FITC–BSA, RhB was much easier to diffuse out of the silk particles, which could be the secondary reason of relatively lower encapsulation efficiency. Last but not least, proteins such as BSA and silk were both negative charged materials, they were supposed to strongly expel against each other and bring low encapsulation efficiencies. However, experimental data shown that the high molecular as well as hydrophobic affinities of model drugs with silk molecular led to high encapsulation efficiency compared with the effects of molecular weight. As seen in the case of RITC–Dextran, in which tiny amount of RITC–Dextran was loaded in the silk particles, probably due to its hydrophilic property, electrical neutral and diverse structure from silk, although its molecular weight was outstandingly higher than that of RhB.

In confocal microscopy images (Fig. 2d–f), strong green florescence was detected with FITC–BSA loaded particles, indicating strong interactions between FITC–BSA with silk molecular due to high molecular affinities in the particles which retarded release of FITC–BSA. RhB had very strong red florescence distributed evenly in silk particles, due to binding of RhB to silk molecular via hydrophobic interactions and electrostatic attractions. For the RITC–Dextran, the red florescence was weak which proved that few drugs were captured in the silk particles.

### 3.2.2. Release

Fig. 3a shows that extended release profiles could be obtained by loading more FITC–BSA in the silk particles. For example, when the actual loading was 0.27%, the FITC–BSA released faster (up to 100% total release in the fifth day). Significantly, when the actual loading was increased to 4.25%, 10.91% and 13.34% gradually, the release profiles became increased gradually, with the total release of FITC–BSA at 71.92%, 23.65% and 22.48% respectively, after 50 days. However, the encapsulation efficiency for higher loading of FITC–BSA was going down magnificently, supported by the data in Fig. 2. Fig. 3b shows the almost immediate release of RITC–Dextran released, up to 100% total release in 6 h, due to its hydrophilic property and lack of special interactions with the silk fibroin. RhB as hydrophobic positive charged model drug, could attach to silk fibroin via electrostatic and hydrophobic interactions which slowed down the release rate compared with that of hydrophilic electrically neutral RITC–Dextran. Lower loading of RhB (0.153%) could continue to release for 3 h, higher loading (11.99%) could sustain release for prolong period. The highest loading of RhB (11.99%) released faster (33.82% RhB released out in 50 days) than that of FITC–BSA (loading: 13.34% and 10.91%), indicates that FITC–BSA had stronger molecular interactions with silk fibroin. Furthermore, for both FITC–BSA and RhB (hydrophobic substances), along with increase actual loading in silk fibroin particles, their release time extended significantly, although their encapsulation efficiency went down accordingly, as can be seen in Figs. 2 and 3, contrary to the loading and release of hydrophilic drug RITC–Dextran.

### 3.2.3. Release kinetic

Several models were used to simulate the in vitro release profiles, calculated data is presented in Table 1. From the adjusted coefficient of determination, it appeared that the Korsmeyer–Peppas model probably was the best fitting model. The values of n for spheres were <0.43 or 0.43 for Fickian release and 0.85 for case II or zero-order release in this model. For systems exhibiting case II transport, the dominant mechanism for drug transport was due to polymer matrix relaxation. The value of $n > 0.43$ but <0.85 was considered as anomalous transport (non-Fickian) and referred to the coupling of Fickian diffusion and polymer matrix relaxation. The value of $n > 0.85$ was considered as super case II transport (Arifin et al., 2006; Siepmann and Siepmann, 2008). Along with the loading of BSA going up, their release kinetic changed from anomalous transport to Fickian release. This phenomenon was probably caused by less BSA in contact with silk fibroin, and when the water penetrated through the silk fibroin matrix which caused swelling and accelerated the release of BSA. Once the loading of BSA was increase significantly, beside interactions between BSA and silk fibroin, self aggregation of BSA would diminish the contribution of swelling effect of silk fibroin matrix on its release.

As positive charged small molecule, more RhB may bind to the negatively charged silk fibroin. Polymer matrix relaxation would influence its release property, however this effect was not dominant probably due to silk fibroin relaxation, as small molecular RhB could still bind to the negative charged silk fibroin, and Fickian diffusion was dominant. As the RITC–Dextran was hydrophilic electrically neutral high molecular weight polysaccharide, it neither had strong molecular interactions with silk fibroin matrix, nor aggregated in the silk fibroin matrix (low encapsulation efficiency and actual loading). Therefore, the release of RITC–Dextran would be influenced much more significantly by polymer matrix relaxation than that of any other factors.

**Table 1**
Evaluation of the dissolution kinetics of BSA, RhB and RITC–Dextran loaded silk particles according to Higuchi, Korsmeyer–Peppas and Weibull models. $T_{25}$ represented the time necessary to dissolve 25% of the loaded materials; o$T_{25}$, observed $T_{25}$; p$T_{25}$, predicted $T_{25}$; d, day and h, hour.

| Sample | o$T_{25}$ | Higuchi | | | Korsmeyer–Peppas | | | Weibull | | |
|---|---|---|---|---|---|---|---|---|---|---|
| | | $K_H$ | $R_{sqr-adj}$ | p$T_{25}$ | $n$ | $R_{sqr-adj}$ | p$T_{25}$ | $b$ | $R_{sqr-adj}$ | p$T_{25}$ |
| 0.27% BSA | 0.292 d | 40.086 | 0.9156 | 0.322 d | 0.448 | 0.9003 | 0.245 d | 0.851 | 0.8359 | 0.516 d |
| 4.25% BSA | 8.3 d | 10.144 | 0.9873 | 6.074 d | 0.525 | 0.9883 | 6.532 d | 0.776 | 0.9864 | 6.852 d |
| 10.19% BSA | 59.1 d | 3.75 | 0.7765 | 44.435 d | 0.312 | 0.9871 | 59.156 d | 0.368 | 0.9878 | 58.541 d |
| 13.34% BSA | 71.9 d | 3.549 | 0.8622 | 49.619 d | 0.341 | 0.9903 | 65.068 d | 0.383 | 0.9906 | 65.762 d |
| 11.99% RhB | 9.8 d | 6.272 | −0.1719 | 15.886 d | 0.213 | 0.9935 | 10.123 d | 0.356 | 0.9941 | 10.114 d |
| RITC–Dextran | 0.583 h | 40.139 | 0.992 | 0.388 h | 0.555 | 0.9986 | 0.49 h | 1.084 | 0.9659 | 0.701 h |

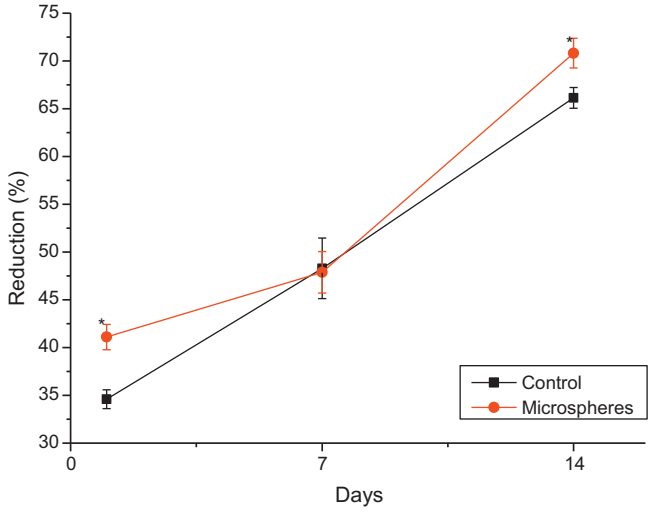


**Fig. 4.** Alamar Blue assay showing superior cell viability on silk particles group compared with control group (*$p < 0.001$, Student's $t$-test).

### 3.3. Cytocompatibility

#### 3.3.1. Alamar Blue assay

In Fig. 4, Alamar Blue assay showed significant increase of cell viability in control and particles groups during the second week of osteoblast culture. Osteoblasts cultured with silk particles showed higher cell viability (by 4.68%) than that of the control group. Based on the data presented, optimistic effects on stimulation of cell viability by silk particles, instead of restrictions on their growth could be concluded. Protein based structure and hydrophobic domain were friendly to cell interactions and growth. Therefore, the silk particles in the culture medium could act as protein carrier surrounding cells, and provided more nutrition and stimulation for cell proliferation. This was the explanation we proposed for higher Alamar Blue reduction when osteoblasts were cultured with silk particles.

#### 3.3.2. Microscopy image

Osteoblasts were observed under fluorescent microcopy after 24 h co-culture with RhB and FITC–BSA loaded silk fibroin particles. Fig. 5a–f shows the evident of RhB and FITC–BSA molecule being transferred into the cells, and the attachment between particles and cell was stable even after three PBS washes. Therefore, good delivery of hydrophobic and protein drugs to osteoblasts could be mediated by the silk particles. The fluorescence intensity of FITC–BSA in the cells was weaker than that of RhB, probably due to higher molecular weight of FITC–BSA corresponding to fewer amounts of BSA molecules in the cells compared to that of RhB.

#### 3.3.3. Flow cytometry

Osteoblasts had been exposed to RhB and FITC–BSA loaded silk fibroin particles for 24 h, and was examined by flow cytometry.

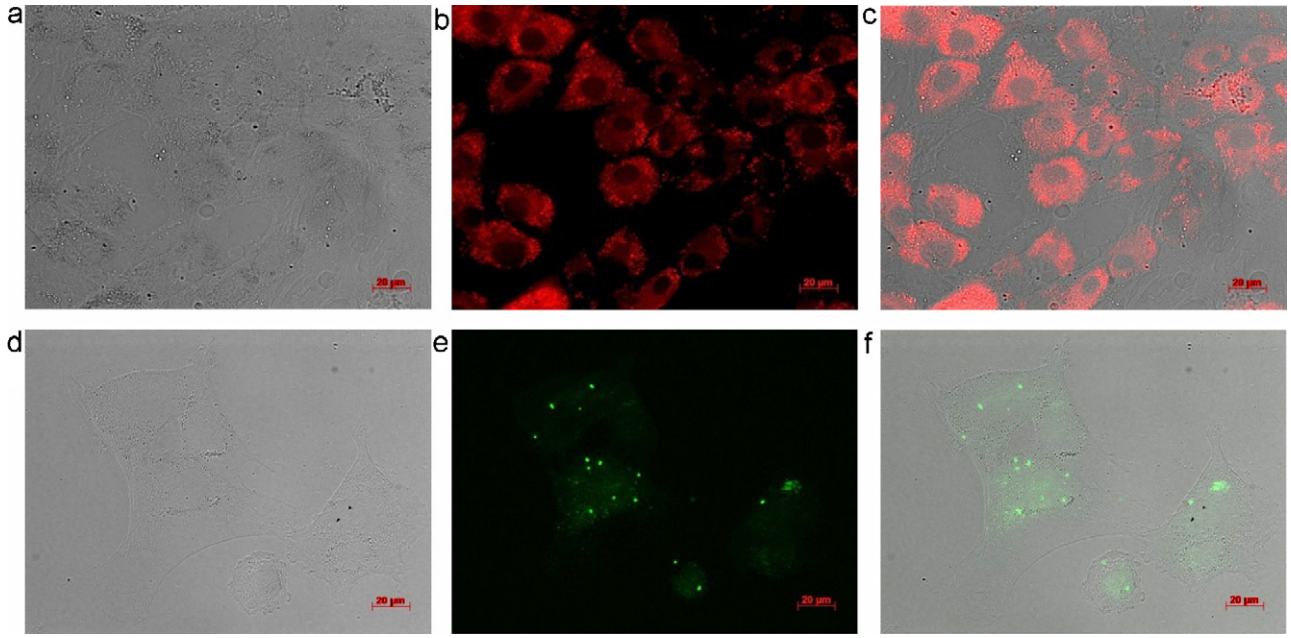


**Fig. 5.** Cellular uptake of RhB (a–c), FITC–BSA (d–f) loaded silk fibroin particles after 24 h: (a) and (d), under bright field; (b) and (e), under fluorescence; (c) and (f), overlay image. Scale bar = 20 μm.

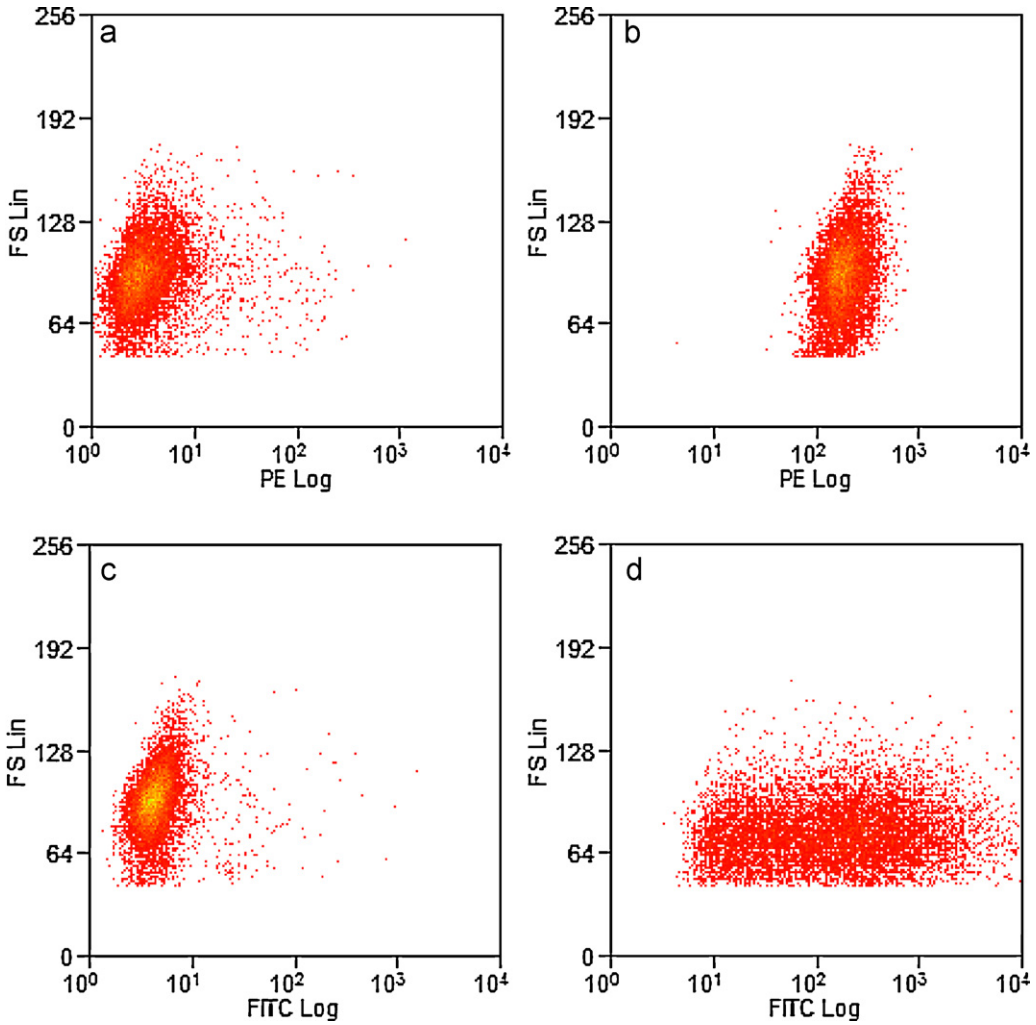


**Fig. 6.** Association of osteoblasts with RhB and FITC–BSA loaded silk fibroin particles measured by flow cytometry (10,000 events): untreated cells (a and c), cells cultured with RhB loaded particles (b) and cells cultured with FITC–BSA loaded particles (d).

Obvious enhancement of fluorescence intensity of cells in both groups after interactions with RhB and FITC–BSA loaded silk fibroin particles is shown in Fig. 6a–d. Hence, the silk fibroin particles could be very efficient carriers for loading and delivery of hydrophobic and protein drugs to cells. More uniform fluorescence increase was observed on cells incubated with RhB loaded silk fibroin particles probably caused by higher burst release (actual loading: 11.99% and burst release: 14.13%) and lower molecular weight of RhB than that of FITC–BSA.

## 4. Conclusion

In this article, silk fibroin particles with average size of 980 nm were prepared. And the particles showed good property for loading and release of hydrophobic drugs as well as protein model drugs. Moreover, benign cytocompatibility was also found when these particles were cultured with osteoblasts. Most importantly, the silk fibroin particles had amazing ability to deliver drugs to cells, most cells were happy to accept the particles as well as the drugs in the particles. Hence, the silk fibroin particles could be potential candidate for application in controlled release and pharmaceutics.

## Acknowledgements

This research was supported by the Biomedical Research Council, Singapore (Grant No. R-175-000-086-305). The authors also wish to thank Dr. Yang Zheng for proof reading.

## References

Arifin, D.Y., Lee, L.Y., Wang, C.H., 2006. Mathematical modeling and simulation of drug release from microspheres: implications to drug delivery systems. Adv. Drug Deliv. Rev. 58, 1274–1325.
Baimark, Y., Srihanam, P., Srisuwan, Y., Phinyocheep, P., 2010. Preparation of porous silk fibroin microparticles by a water-in-oil emulsification-diffusion method. J. Appl. Polym. Sci. 118, 1127–1133.
Breslauer, D.N., Muller, S.J., Lee, L.P., 2010. Generation of monodisperse silk microspheres prepared with microfluidics. Biomacromolecules 11, 643–647.
Cao, X.Y., Yin, M.Z., Zhang, L.N., Li, S.P., Cao, Y., 2006. Establishment of a new model for culturing rabbit osteoblasts in vitro. Biomed. Mater. 1, L16–L19.
Cao, Z.B., Chen, X., Yao, J.R., Huang, L., Shao, Z.Z., 2007. The preparation of regenerated silk fibroin microspheres. Soft Matter 3, 910–915.
Costa, P., Manuel, J., Lobo, S., 2001. Modeling and comparison of dissolution profiles. Eur. J. Pharm. Sci. 13, 123–133.
Fan, H.B., Liu, H.F., Toh, S.L., Goh, J.C.H., 2009. Anterior cruciate ligament regeneration using mesenchymal stem cells and silk scaffold in large animal model. Biomaterials 30, 4967–4977.
Hofmann, S., Foo, C., Rossetti, F., Textor, M., Vunjak-Novakovic, G., Kaplan, D.L., Merkle, H.P., Meinel, L., 2006. Silk fibroin as an organic polymer for controlled drug delivery. J. Control. Release 111, 219–227.

Lammel, A.S., Hu, X., Park, S.H., Kaplan, D.L., Scheibel, T.R., 2010. Controlling silk fibroin particle features for drug delivery. Biomaterials 31, 4583–4591.
Mathur, A.B., Gupta, V., 2010. Silk fibroin-derived nanoparticles for biomedical applications. Nanomedicine 5, 807–820.
Min, B.M., Lee, G., Kim, S.H., Nam, Y.S., Lee, T.S., Park, W.H., 2004. Electrospinning of silk fibroin nanofibers and its effect on the adhesion and spreading of normal human keratinocytes and fibroblasts in vitro. Biomaterials 25, 1289–1297.
Schacht, E., Toncheva, V., Vandertaelen, K., Heller, J., 2006. Polyacetal and poly(ortho ester)-poly(ethylene glycol) graft copolymer thermogels: preparation, hydrolysis and FITC–BSA release studies. J. Control. Release 116, 219–225.
Shi, P.J., Zuo, Y., Zou, Q., Shen, J., Zhang, L., Li, Y.B., Morsi, Y.S., 2009. Improved properties of incorporated chitosan film with ethyl cellulose microspheres for controlled release. Int. J. Pharm. 375, 67–74.
Siepmann, J., Siepmann, F., 2008. Mathematical modeling of drug delivery. Int. J. Pharm. 364, 328–343.
Slotta, U.K., Rammensee, S., Gorb, S., Scheibel, T., 2008. An engineered spider silk protein forms microspheres. Angew. Chem. Int. Ed. Engl. 47, 4592–4594.
Srisuwan, Y., Srihanam, P., Baimark, Y., 2009. Preparation of silk fibroin microspheres and its application to protein adsorption. J. Macromol. Sci. Pure 46, 521–525.
Wang, X.Q., Wenk, E., Matsumoto, A., Meinel, L., Li, C.M., Kaplan, D.L., 2007. Silk microspheres for encapsulation and controlled release. J. Control. Release 117, 360–370.
Wang, X.Q., Yucel, T., Lu, Q., Hu, X., Kaplan, D.L., 2010. Silk nanospheres and microspheres from silk/pva blend films for drug delivery. Biomaterials 31, 1025–1035.
Wenk, E., Wandrey, A.J., Merkle, H.P., Meinel, L., 2008. Silk fibroin spheres as a platform for controlled drug delivery. J. Control. Release 132, 26–34.
Weska, R.F., Nogueira, G.M., Vieira, W.C., Beppu, M.M., 2009. Porous silk fibroin membrane as a potential scaffold for bone regeneration. In: Prado, M., Zavaglia, C. (Eds.), Bioceramics, 21, pp. 187–190.
Zhao, Y., Chen, J., Chou, A.H.K., Li, G., LeGeros, R.Z., 2009. Nonwoven silk fibroin net/nano-hydroxyapatite scaffold: preparation and characterization. J. Biomed. Mater. Res. A 91A, 1140–1149.